Chapter 10

Left Ventricular Muscle and Fluid Mechanics in Acute Myocardial Infarction

Gaetano Nucifora, Victoria Delgado, Matteo Bertini, Nina Ajmone Marsan, Nico R. Van de Veire, Arnold C.T. Ng, Hans-Marc J. Siebelink, Martin J. Schalij, Eduard R. Holman, Partho P. Sengupta, Jeroen J. Bax

Am J Cardiol 2010;106:1404–1409

ABSTRACT

Left ventricular (LV) diastolic filling is characterized by the formation of intraventricular rotational bodies of fluid (termed "vortex rings") that optimize the efficiency of LV ejection. The aim of the present study was to evaluate the morphology and dynamics of LV diastolic vortex ring formation early after acute myocardial infarction (AMI), in relation to LV diastolic function and infarct size. A total of 94 patients with a first ST-segment elevation AMI (59±11 years; 78% men) were included. All patients underwent primary percutaneous coronary intervention. After 48 hours, the following examinations were performed: 2-dimensional echocardiography with speckle-tracking analysis to assess the LV systolic and diastolic function, the vortex formation time (VFT, a dimensionless index for characterizing vortex formation), and the LV untwisting rate; contrast echocardiography to assess LV vortex morphology; and myocardial contrast echocardiography to identify the infarct size. Patients with a large infarct size (≥3 LV segments) had a significantly lower VFT ($p < 0.001$) and vortex sphericity index ($p < 0.001$). On univariate analysis, several variables were significantly related to the VFT, including anterior AMI, LV end-systolic volume, LV ejection fraction, grade of diastolic dysfunction, LV untwisting rate, and infarct size. On multivariate analysis, the LV untwisting rate ($\beta = -0.43$, $p < 0.001$) and infarct size ($\beta = -0.33$, $p = 0.005$) were independently associated with VFT. In conclusion, early in AMI, both the LV infarct size and the mechanical sequence of diastolic restoration play key roles in modulating the morphology and dynamics of early diastolic vortex ring formation.

INTRODUCTION

The assessment of left ventricular (LV) diastolic function usually relies on noninvasive measures of LV relaxation and stiffness.[1] More recently, the evaluation of LV muscle and fluid mechanics, using novel echocardiographic indexes and techniques, has been proposed to refine the assessment of LV diastolic function.[2-5] In particular, 2-dimensional speckle tracking imaging enables the assessment of the complex torsional mechanics of the left ventricle. During systole, the contraction of the helically arranged subendocardial and subepicardial layers leads to the opposite rotation of the LV apex and LV base, the so-called LV twist.[3,6] During isovolumic relaxation, the reverse rotation of the LV apex and LV base (LV untwisting) releases the energy stored during LV systole. The restoring forces generate intraventricular pressure gradients contributing to early LV filling.[3,6,7] These complex LV mechanics are associated with characteristic intraventricular fluid dynamics.[4,8] During early LV filling, the blood flow forms intraventricular rotational bodies of fluid (so-called vortex rings) that are critical in optimizing the blood flow during LV ejection.[4,8] These diastolic fluid dynamics can be noninvasively evaluated using color Doppler echocardiography or contrast echocardiography.[9] In addition, a novel echocardiographic dimensionless index (vortex formation time [VFT]) has recently been introduced to quantitatively characterize the optimal conditions leading to vortex formation.[5]

It is well known that myocardial injuries, such as those induced by acute myocardial infarction (AMI), negatively affect the LV diastolic function;[10] conversely, not much data regarding the effect of AMI on the VFT or vortex morphology are available. The knowledge of abnormalities involving the LV vortex formation in clinical setting would be useful, because it would provide direct information regarding the ultimate goal of LV performance (i.e., optimal blood flow). Accordingly, the aim of the present study was to quantify vortex ring formation using the dimensionless index of the VFT and to estimate the morphology of the

vortex during routine contrast echocardiography early after AMI. In addition, we sought to correlate the dynamics of vortex ring formation with LV diastolic function, torsional mechanics, and the extent of myocardial damage (i.e., infarct size).

METHODS

The population consisted of 110 consecutive patients admitted to the coronary care unit for a first ST-segment elevation AMI. The diagnosis of AMI was determined from typical electrocardiographic changes and/or ischemic chest pain associated with the elevation of cardiac biomarkers.[11] All patients underwent immediate coronary angiography and primary percutaneous coronary intervention. The infarct-related artery was identified by the site of coronary occlusion during coronary angiography and electrocardiographic criteria.

The clinical evaluation included 2-dimensional echocardiography with speckle-tracking analysis to assess the LV systolic and diastolic function, dimensionless index of VFT (see paragraph with equation below), and LV untwisting rate; contrast echocardiography to assess LV vortex morphology; and myocardial contrast echocardiography (MCE) to assess the extent of perfusion abnormalities and infarct size. These echocardiographic examinations were performed 48 hours after primary percutaneous coronary intervention. Subsequently, the relations between VFT and vortex morphology with LV diastolic function, LV untwisting rate, and infarct size (as assessed from MCE) were evaluated.

Patients with significant (moderate or severe) valvular heart disease or rhythm other than sinus were not included.

The local ethical committee approved the study protocol, and all patients provided informed consent.

All patients with AMI underwent imaging in the left lateral decubitus position using a commercially available system (Vivid 7 Dimension, GE Healthcare, Horten, Norway) equipped with a 3.5-MHz transducer.

Standard 2-dimensional images and Doppler and color Doppler data were acquired from the parasternal and apical views (2-, 3- and 4-chamber) and digitally stored in cine-loop format. The analyses were subsequently performed off-line using EchoPAC, version 7.0.0 (GE Healthcare, Horten, Norway). The LV end-diastolic and end-systolic volumes were measured according to the Simpson's biplane method, and the LV ejection fraction was calculated as [(end-diastolic volume − end-systolic volume)/end-diastolic volume] × 100.[12]

As previously reported,[1] transmitral and pulmonary vein pulsed-wave Doppler tracings were used to classify the diastolic function as normal, diastolic dysfunction grade 1 (mild), diastolic dysfunction grade 2 (moderate), diastolic dysfunction grade 3 (severe), or diastolic dysfunction grade 4 (severe).

The VFT, a dimensionless index that characterizes the optimal conditions for vortex formation during diastole was calculated as follows:[5,13]

$$VFT = \frac{4(1-\beta)}{\pi D^3} \times SV$$

where SV is the stroke volume, β the fraction of stroke volume contributed from the atrial component of LV filling and calculated from Doppler spectra of the E and A waves, and D the mitral valve diameter in centimeters. The mitral valve diameter was obtained by averaging the largest mitral orifice diameters measured during early diastolic filling in the 2-, 3-, and 4-chamber apical views.

Speckle tracking analysis was applied to evaluate the LV untwisting rate. Parasternal short-axis images of the left ventricle were acquired at 2 different levels: the basal level, identified by the mitral valve and the apical level, identified as the smallest cavity achievable distally to the papillary muscles (moving the probe down and slightly laterally, if needed). The frame rate was 60 to 100 frames/s, and 3 cardiac cycles for each short-axis level were stored in cine-loop format for off-line analysis (EchoPAC, version 7.0.0, GE Healthcare). The endocardial border

was traced at an end-systolic frame, and the region of interest was chosen to fit the whole myocardium. The software allows the operator to check and validate the tracking quality and to adjust the endocardial border or modify the width of the region of interest, if needed. Each short-axis image was automatically divided into 6 standard segments: septal, anteroseptal, anterior, lateral, posterior, and inferior. The software calculated the LV rotation from the apical and basal short-axis images as the average angular displacement of the 6 standard segments, referring to the ventricular centroid, frame by frame. Counterclockwise rotation was marked as a positive value and clockwise rotation as a negative value when viewed from the LV apex. LV twist was defined as the net difference (in degrees) of the apical and basal rotation at the isochronal points. The opposite rotation after LV twist was defined as the LV untwist and the time derivative of the LV untwist was defined as the LV untwisting rate (° /s).

Immediately after 2-dimensional echocardiography, contrast echocardiography was performed using the same ultrasound system. Luminity (Bristol-Myers Squibb Pharma, Brussels, Belgium) was used as the contrast agent. A slow intravenous bolus of echocardiographic contrast (0.1 to 0.2 ml) was administered, followed by 1 to 3 ml of normal saline flush.[4] Apical 3- and 4-chamber views were acquired using a low-power technique (0.1 to 0.4 mechanical index), and the focus was set in the middle of the left ventricle. The machine settings were optimized to obtain the best possible visualization of LV vortex formation. The frame rate was 60 to 100 frames/s, and ≥3 cardiac cycles were stored in cine-loop format for off-line analysis (EchoPAC, version 7.0.0, GE Healthcare). For the evaluation of vortex morphology, the vortex length and width relative to the LV volume were measured during early diastolic filling in the apical 3-chamber view. A vortex sphericity index was calculated as the vortex length/vortex width ratio.

Immediately after contrast echocardiography, MCE was performed to evaluate myocardial perfusion to assess the infarct size after AMI. The

same ultrasound system was used, and the 3 standard apical views were acquired using a low-power technique (0.1 to 0.26 mechanical index). The background gains were set such that minimal tissue signal was seen, and the focus was set at the level of the mitral valve. Luminity (Bristol-Myers Squibb Pharma) was used as the contrast agent. Each patient received an infusion of 1.3 ml of echocardiographic contrast diluted in 50 ml of 0.9% NaCl solution through a 20-gauge intravenous catheter in a proximal forearm vein. The infusion rate was initially set at 4.0 ml/min and then titrated to achieve optimal myocardial enhancement without attenuation artifacts.[14] The machine settings were optimized to obtain the best possible myocardial opacification with minimal attenuation. At least 15 cardiac cycles after high mechanical index (1.7) microbubble destruction were stored in cine-loop format for off-line analysis (EchoPAC, version 7.0.0, GE Healthcare).[15] The left ventricle was divided according to a standard 16-segment model, and a semiquantitative scoring system was used to assess contrast intensity after microbubble destruction:[12] *1*, normal/homogenous opacification; *2*, reduced/patchy opacification; and *3*, minimal or absent contrast opacification.[15,16] A myocardial perfusion index (MPI) was derived by adding the contrast scores of all segments and dividing by the total number of segments.[15,16] In accordance with the number of segments showing minimal or absent contrast opacification, patients were categorized as having a small infarct size (<3 segments with minimal or absent contrast opacification) or a large infarct size (≥3 segments with minimal or absent contrast opacification).[17]

Continues variables are expressed as the mean±SD, when normally distributed, and as the median and interquartile range, when non-normally distributed. Categorical data are presented as absolute numbers and percentages. Differences in continuous variables were assessed using the Student t test or the Mann-Whitney U test, as appropriate. The chi-square test or Fisher's exact test, if appropriate, were computed to assess differences in categorical variables.

Linear regression analyses were performed to evaluate the relation between the VFT and the vortex sphericity index; the vortex parameters and the grade of diastolic dysfunction; the vortex parameters and the LV untwisting rate; and the vortex parameters and infarct size (as assessed from MCE). Univariate and multivariate linear regression analyses (enter model) were performed to evaluate the relation between VFT and the following clinical and echocardiographic variables: age, gender, infarct location (anterior vs nonanterior), multivessel disease, LV end-diastolic volume, LV end-systolic volume, LV ejection fraction, diastolic dysfunction grade, LV untwisting rate, and MPI. Only significant variables on univariate analysis were entered as covariates in the multivariate model. A p value of <0.05 was considered statistically significant. Statistical analysis was performed using the Statistical Package for Social Sciences software package, version 15.0 (SPSS, Chicago, Illinois).

RESULTS

A total of 16 patients were excluded because of suboptimal echocardiographic images that prevented adequate analysis of the speckle-tracking data, vortex morphology, or myocardial perfusion. The clinical characteristics of the 94 patients included in the study are listed in Table 1, and the echocardiographic characteristics are listed in Table 2. The mean LV ejection fraction was $47 \pm 10\%$. Most (54%) had grade 1 diastolic dysfunction. From the speckle tracking analysis findings, the diastolic function was characterized by a mean peak untwisting rate of $-94 \pm 32°$ /s. From the LV hydrodynamics evaluation, the VFT was 1.4 ± 0.6, and the vortex sphericity index was 1.1 ± 0.2.

As shown in Figure 1, a good relation between the VFT and vortex sphericity index was observed ($r = 0.61$; $p < 0.001$). Both LV vortex parameters were weakly related to the LV diastolic function (Figure 2). In contrast, good relations between the VFT and the LV untwisting rate ($r =$

0.65; p <0.001) and between the vortex sphericity index and the LV untwisting rate (r = 0.61; p <0.001) were observed (Figure 3).

Table 1. Clinical patient characteristics

Variable	n = 94
Age (years)	59±11
Men	73 (78%)
Diabetes mellitus	12 (13%)
Hypercholesterolemia *	15 (16%)
Hypertension †	37 (39%)
Current or previous smoking	52 (55%)
Anterior wall myocardial infarction	47 (50%)
Infarct-related coronary artery	
- left anterior descending	47 (50%)
- left circumflex	16 (17%)
- right	31 (33%)
Multi-vessel coronary disease	36 (38%)
Peak troponin T (μg/l)	2.9 (1.6-7.5)

Data are expressed as mean±SD or median (interquartile range), and n (%). *: Defined as total cholesterol ≥240 mg/dl. †: Defined as systolic blood pressure ≥140 mmHg and/or diastolic blood pressure ≥90 mmHg.

According to the results from MCE, 69 patients (73%) with AMI had a small infarct size (<3 segments with minimal or absent contrast opacification) and 25 (27%) had a large infarct size (≥3 segments with minimal or absent contrast opacification). The echocardiographic characteristics of these 2 groups are summarized in Table 2. Patients with a small infarct size had a significant greater LV ejection fraction compared to patients with a large infarct size (51±8% vs 39±8%; p <0.001).

No significant difference in the grade of diastolic dysfunction was observed between patients with a small and large infarct size; most of the patients in both groups (52% and 60%, respectively) had grade 1 diastolic dysfunction. However, the LV untwisting rate was significantly impaired in the patients with a large infarct size (−69±27° /s vs −103±29° /s; p <0.001). Regarding the vortex parameters, patients with a large infarct size had a significantly lower VFT (1.0±0.5 vs

1.6±0.5; p <0.001) and vortex sphericity index (0.9±0.2 vs 1.2±0.2; p <0.001). As shown in Figure 4, a good relation between the VFT and MPI (expressing infarct size) (r = 0.63; p <0.001) and between the vortex sphericity index and MPI (r = 0.71; p <0.001) was observed.

Table 2. Echocardiographic characteristics

	All AMI patients (n = 94)	Small infarct (n = 69)	Large infarct (n = 25)	p value
Left ventricular end-diastolic volume (ml)	105±28	104±25	107±36	0.69
Left ventricular end-systolic volume (ml)	56±22	52±18	66±29	0.024
Left ventricular ejection fraction (%)	47±10	51±8	39±8	<0.001
E wave velocity (cm/sec)	62±0.18	62±0.18	62±0.18	0.97
E wave deceleration time (msec)	201±59	207±55	184±67	0.11
A wave velocity (cm/sec)	68±0.17	68±0.13	70±0.25	0.76
Diastolic function				0.18
- grade 0	35 (37%)	29 (42%)	6 (24%)	
- grade 1	51 (54%)	36 (52%)	15 (60%)	
- grade 2	5 (6%)	3 (4%)	2 (8%)	
- grade 3-4	3 (3%)	1 (1%)	2 (8%)	
Untwisting rate (° /sec)	-94±32	-103±29	-69±27	<0.001
Vortex formation time	1.4±0.6	1.6±0.5	1.0±0.5	<0.001
Vortex length/left ventricular volume (cm/ml)	0.02±0.01	0.02±0.01	0.01±0.01	0.19
Vortex width/left ventricular volume (cm/ml)	0.01±0.01	0.01±0.01	0.02±0.01	0.026
Vortex sphericity index	1.1±0.2	1.2±0.2	0.9±0.2	<0.001
Myocardial perfusion index	1.4±0.3	1.2±0.2	1.7±0.3	<0.001

Data are expressed as mean±SD and n (%).

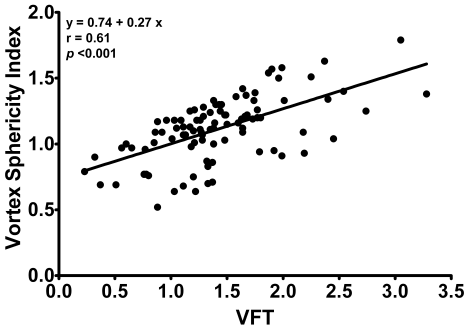

Figure 1. Relation between VFT and vortex sphericity index.

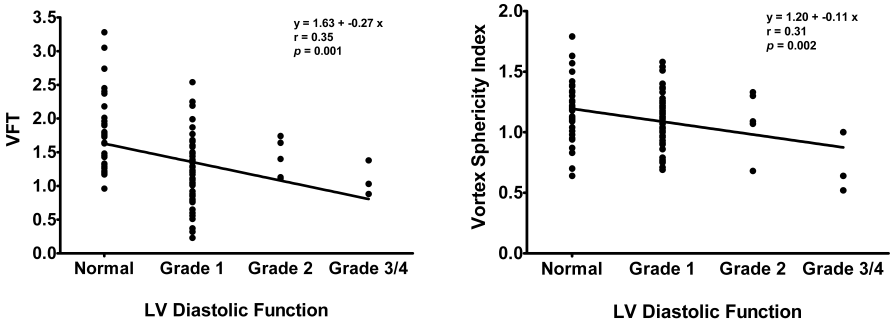

Figure 2. Relation between grades of LV diastolic dysfunction and (**left panel**) VFT and (**right panel**) vortex sphericity index.

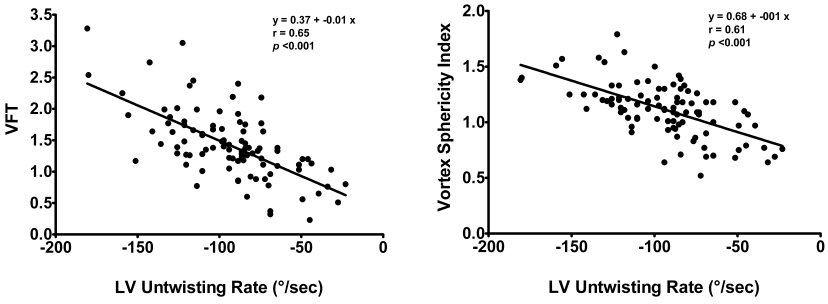

Figure 3. Relation between LV untwisting rate and (**left panel**) VFT and (**right panel**) vortex sphericity index.

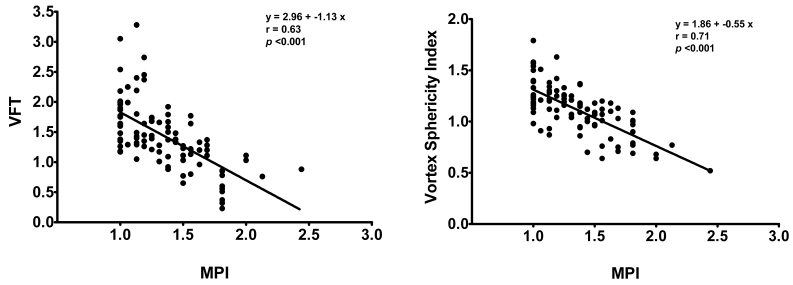

Figure 4. Relation between infarct size (expressed as MPI) and (**left panel**) VFT and (**right panel**) vortex sphericity index.

Table 3 lists the results of the univariate and multivariate linear regression analyses performed to determine the factors related to VFT among patients with AMI. On univariate analysis, several variables were significantly related to VFT, including anterior AMI, LV end-systolic volume, LV ejection fraction, diastolic dysfunction grade, LV untwisting rate, and MPI. On multivariate analysis, only the LV untwisting rate ($\beta = -0.43$, $p < 0.001$) and MPI ($\beta = -0.33$, $p = 0.005$) were independently associated with the VFT.

Table 3. Univariate and multivariate linear regression analyses to determine independent correlates of vortex formation time (VFT)

	Univariate		Multivariate	
	β	**p value**	**β**	**p value**
Age	-0.16	0.12	-	-
Men	-0.024	0.82	-	-
Anterior myocardial infarction	-0.37	<0.001	-0.059	0.49
Multi-vessel disease	-0.15	0.16	-	-
Left ventricular end-diastolic volume	0.065	0.53	0.18	0.62
Left ventricular end-systolic volume	-0.21	0.039	0.053	0.91
Left ventricular ejection fraction	0.53	<0.001	0.092	0.70
Grade of diastolic dysfunction	-0.35	0.001	-0.081	0.31
Untwisting rate	-0.65	<0.001	-0.43	<0.001
Myocardial perfusion index	-0.63	<0.001	-0.33	0.005

Abbreviations as in Table 2.

DISCUSSION

The results of the present study can be summarized as follows: both the VFT and the vortex sphericity index were weakly related to global LV diastolic function, and a good relation was observed between the LV vortex parameters and LV untwisting rate. Second, both the VFT and the vortex sphericity index had a good relation with infarct size (as assessed by MCE), indicating progressive impairment of LV diastolic fluid dynamics with an increasing extent of myocardial damage. Finally, on multivariate analysis, a significant independent relation was observed between VFT and both the LV untwisting rate and the MPI.

Several investigators have previously demonstrated the process of vortex formation during LV filling using numeric or physical models and flow visualization techniques (i.e., cardiac magnetic resonance imaging, color Doppler echocardiography, and MCE) in clinical studies.[4,8,9,18-21] The process of vortex formation starts immediately after the onset of the early diastolic phase, lasting the whole diastolic period.[4] It is related to the difference in velocity between the high-speed inflow jet after mitral valve opening and the surrounding still fluid in the left ventricle. The shear layer between the moving and the still part of the blood promotes a natural swirling of flow inside the left ventricle, leading to the vortex formation.[4,22]

The LV vortex has been shown to optimize the diastolic fluid dynamics and the efficiency of systolic ejection of blood. The LV vortex redirects the blood flow from the LV base to the LV apex during isovolumic relaxation and toward the LV outflow tract and aorta during isovolumic contraction.[4,22,23] In addition, the LV vortex constitutes a kinetic energy reservoir (storing the kinetic energy of the high-speed inflow jet) and, consequently, enhances the ejection of blood during systole.[24] The premature loss or absence of diastolic LV vortex would conversely lead to the dissipation of the stored kinetic energy, resulting in an increased myofiber cardiac work and oxygen demand.[24]

In the present study, the effect of AMI on LV vortex flow was assessed. In particular, the morphology of the intraventricular vortex was evaluated using contrast echocardiography. In addition, the dimensionless index of VFT was also evaluated. The VFT is a recently proposed parameter for characterizing the process of vortex ring formation.[5] It is a measure of the length/diameter ratio of the fluid column and is directly proportional to the time-averaged velocity of flow through the mitral valve and inversely proportional to the mitral valve size.[5] A previous in vitro study showed that a range of VFT from 3.3 to 4.5 characterizes the optimal hemodynamic conditions for vortex ring formation.[5]

A good linear relation was observed between the vortex sphericity index and the VFT, indicating that suboptimal hemodynamic conditions for vortex ring formation (i.e., low values of VFT) are associated with short and wide LV vortex rings. In addition, both the VFT and the vortex sphericity index were weakly related to the global LV diastolic function, and a good relation was observed between the LV vortex parameters and LV untwisting rate. This finding suggests that LV hydrodynamics are mainly related to LV diastolic suction rather than to global LV diastolic function. Suction gradients are necessary for the redirection of flow from the LV base to the LV apex and, consequently, for vortex ring formation. In addition, suction gradients are mainly determined by the LV untwisting mechanics.[7] Reduced LV untwisting after AMI might attenuate these suction gradients, leading finally to abnormal LV vortex ring formation.

In the present study, the relation between LV vortex flow and infarct size was also evaluated. Both the VFT and the vortex sphericity index had a significant linear relation with infarct size (as assessed by MCE), indicating that larger infarctions are associated with a more severe alteration in LV intracavitary blood flow dynamics. This finding is in line with the study by Hong et al,[4] showing abnormal LV vortex morphology among patients with reduced LV systolic function compared to normal controls. As a consequence of impaired VFT and abnormal vortex morphology, the relative stasis and delay or modification of the normal blood flow during

the cardiac cycle might occur, predisposing to LV thrombus formation.[9] Moreover, taking into account the essential role of LV vortex rings in optimizing the ejection of blood during systole, a significant impairment of LV vortex ring formation might contribute to a progressive decrease in LV systolic function.[24] However, follow-up studies that also include other parameters of diastolic function (e.g., tissue-Doppler parameters, isovolumic relaxation time, and time of untwisting) are needed to demonstrate the prognostic role of LV hydrodynamics parameters for the prediction of post-AMI complications and outcome.

REFERENCES

1. Lester SJ, Tajik AJ, Nishimura RA, et al. Unlocking the mysteries of diastolic function: deciphering the Rosetta Stone 10 years later. J Am Coll Cardiol. 2008; 51: 679–689

2. Thomas JD, Popovic, ZB. Assessment of left ventricular function by cardiac ultrasound. J Am Coll Cardiol. 2006; 48: 2012–2025

3. Sengupta PP, Khandheria BK, Narula, J. Twist and untwist mechanics of the left ventricle. Heart Fail Clin. 2008; 4: 315–324

4. Hong GR, Pedrizzetti G, Tonti G, et al. Characterization and quantification of vortex flow in the human left ventricle by contrast echocardiography using vector particle image velocimetry. JACC Cardiovasc Imaging. 2008; 1: 705–717

5. Gharib M, Rambod E, Kheradvar A, et al. Optimal vortex formation as an index of cardiac health. Proc Natl Acad Sci USA. 2006; 103: 6305–6308

6. Bertini M, Nucifora G, Ajmone Marsan N, et al. Left ventricular rotational mechanics in acute myocardial infarction and in chronic (ischemic and non-ischemic) heart failure patients. Am J Cardiol. 2009; 103: 1506–1512

7. Burns AT, La Gerche A, Prior DL, et al. Left ventricular untwisting is an important determinant of early diastolic function. JACC Cardiovasc Imaging. 2009; 2: 709–716

8. Kim WY, Walker PG, Pedersen EM, et al. Left ventricular blood flow patterns in normal subjects: a quantitative analysis by three-dimensional magnetic resonance velocity mapping. J Am Coll Cardiol. 1995; 26: 224–238

9. Sengupta PP, Burke R, Khandheria BK, et al. Following the flow in chambers. Heart Fail Clin. 2008; 4: 325–332

10. Popovic AD. Old and new paradigms on diastolic function in acute myocardial infarction. Am Heart J. 1999; 138: S84–S88
11. Thygesen K, Alpert JS, White HD, et al. Universal definition of myocardial infarction. Circulation. 2007; 116: 2634–2653
12. Lang RM, Bierig M, Devereux RB, et al. Recommendations for chamber quantification: a report from the American Society of Echocardiography's Guidelines and Standards Committee and the Chamber Quantification Writing Group, developed in conjunction with the European Association of Echocardiography, a branch of the European Society of Cardiology. J Am Soc Echocardiogr. 2005; 18: 1440–1463
13. Jiamsripong P, Calleja AM, Alharthi MS, et al. Impact of acute moderate elevation in left ventricular afterload on diastolic transmitral flow efficiency: analysis by vortex formation time. J Am Soc Echocardiogr. 2009; 22: 427–431
14. Weissman NJ, Cohen MC, Hack TC, et al. Infusion versus bolus contrast echocardiography: a multicenter, open-label, crossover trial. Am Heart J. 2000; 139: 399–404
15. Dwivedi G, Janardhanan R, Hayat SA, et al. Prognostic value of myocardial viability detected by myocardial contrast echocardiography early after acute myocardial infarction. J Am Coll Cardiol. 2007; 50: 327–334
16. Main ML, Magalski A, Kusnetzky LL, et al. Usefulness of myocardial contrast echocardiography in predicting global left ventricular functional recovery after anterior wall acute myocardial infarction. Am J Cardiol. 2004; 94: 340–342
17. Caldas MA, Tsutsui JM, Kowatsch I, et al. Value of myocardial contrast echocardiography for predicting left ventricular remodeling and segmental functional recovery after anterior wall acute myocardial infarction. J Am Soc Echocardiogr. 2004; 17: 923–932
18. Bellhouse BJ. Fluid mechanics of a model mitral valve and left ventricle. Cardiovasc Res. 1972; 6: 199–210
19. Baccani B, Domenichini F, Pedrizzetti G, et al. Fluid dynamics of the left ventricular filling in dilated cardiomyopathy. J Biomech. 2002; 35: 665–671
20. Steen T, Steen S. Filling of a model left ventricle studied by colour M mode Doppler. Cardiovasc Res. 1994; 28: 1821–1827
21. Vierendeels JA, Riemslagh K, Dick E, et al. Computer simulation of intraventricular flow and pressure gradients during diastole. J Biomech Eng. 2000; 122: 667–674

22. Domenichini F, Pedrizzetti G, Baccani B. Three-dimensional filling flow into a model left ventricle. J Fluid Mech. 2005; 539: 179–198
23. Sengupta PP, Khandheria BK, Korinek J, et al. Left ventricular isovolumic flow sequence during sinus and paced rhythms: new insights from use of high-resolution Doppler and ultrasonic digital particle imaging velocimetry. J Am Coll Cardiol. 2007; 49: 899–908
24. Pedrizzetti G, Domenichini F. Nature optimizes the swirling flow in the human left ventricle. Phys Rev Lett. 2005; 95: 108101